

# Pyrolysis kinetics and activation thermodynamic parameters of exhausted coffee residue and coffee husk using thermogravimetric analysis

Alivia Mukherjee<sup>1</sup> | Jude A. Okolie<sup>1</sup> | Ramani Tyagi<sup>1,2</sup> | Ajay K. Dalai<sup>1</sup> | Catherine Niu<sup>1</sup>

<sup>1</sup>Department of Chemical and Biological Engineering, University of Saskatchewan, Saskatoon, Saskatchewan, Canada

<sup>2</sup>Department of Chemical Engineering, University of Michigan, Ann Arbor, Michigan

## Correspondence

Ajay K. Dalai, Department of Chemical and Biological Engineering, University of Saskatchewan, Saskatoon, Saskatchewan, Canada.

Email: [ajay.dalai@usask.ca](mailto:ajay.dalai@usask.ca)

## Funding information

Canada Research Chairs; Natural Sciences and Engineering Research Council of Canada

## Abstract

Exhausted coffee residue (ECR) and coffee husk (CH) are potential feedstock for energy production through thermochemical and biochemical conversion processes. Kinetic study of ECR and CH is essential for the design and optimization of different thermochemical conversion processes. In this study, four different iso-conversional methods were employed in the estimation of the activation energy ( $E_A$ ) and pre-exponential factor ( $A$ ). The methods used includes Flynn-Wall-Ozawa (FWO), Kissinger-Akahira-Sunose (KAS), Kissinger's method, and the Friedman method. Data from the thermogravimetric/derivative thermogravimetric analysis (TGA/DTG) at varying heating rates of 5-20°C/min in an inert environment were used in this study. It was observed that the heating rate influences the pyrolysis parameters such as peak temperature, maximum degradation rate and initial decomposition temperature. The activation energy for ECR using the FWO method was in the range of 62.3-102.4 kJ · mol<sup>-1</sup>. Likewise, the KAS and Friedman methods yielded activation energy between 51.3-93.3 kJ · mol<sup>-1</sup> and 10.6-122.7 kJ · mol<sup>-1</sup>, respectively. In addition, the activation energy calculated for CH using FWO, KAS, and Friedman methods were shown to range from 39.1-140.6 kJ · mol<sup>-1</sup>, 27.7-131.6 kJ · mol<sup>-1</sup>, and 24.9-111.2 kJ · mol<sup>-1</sup>, respectively.

## KEYWORDS

coffee husk, exhausted coffee residues, kinetics, pyrolysis, thermogravimetry

## 1 | INTRODUCTION

Coffee husk (CH) is the dried coffee skin that is left behind during coffee roasting, while coffee pulp (CP) is obtained during the wet coffee processing.<sup>[1]</sup> On the other hand, exhausted coffee residue (ECR) is generated from the coffee brewing process through the production of instant coffee with hot water. For every tonne (t) of fresh coffee consumed annually, about 0.18 t of CH and 0.5 t of

CP are generated. Additionally, the annual production of ECR is estimated at six million tonnes worldwide.<sup>[2]</sup> Reducing coffee by-products presents a severe environmental challenge. On the other hand, the residues generated from the coffee industry could be utilized as feedstocks for diverse applications. For instance, coffee residues can be used as feedstocks for biofuels and biochemical production, as a fertilizer, dietary fibre, and for the production of bioactive compounds.<sup>[3]</sup>

With rapid industrialization and urbanization as a result of population growth, coupled with decreasing fossil fuels reserve, there is an urgent demand to develop alternative and sustainable energy sources. Renewable energy resources such as wind, biomass, and solar energy have some advantages over fossil fuels in terms of their environmentally friendly nature. Unlike other renewable energy resources, biomass can produce liquid and gaseous transportation fuels.<sup>[4]</sup> Furthermore, biomass is widely available and a cheap source of renewable energy. Coffee residues are examples of waste biomass that can be utilized to produce liquid transportation fuels to minimize waste disposal issues and the environmental challenges associated with fossil fuel consumption.

Pyrolysis of coffee residues can be used to produce green fuels and chemical. The process is of interest for the following reasons. First, it can produce solid-residue (char), tar, aqueous phase (aerosols or vapour) and non-condensable gas (syngas) from biomass feedstocks. Secondly, the process is usually carried out in an inert environment (nitrogen or argon).<sup>[5]</sup> Finally, the products obtained from the pyrolysis process can be stored, transported and used as a substitute for fossil-based energy sources.<sup>[6]</sup>

Since pyrolysis product yield and composition is highly dependent on the type and composition of feedstock used together with the experimental conditions used in the degradation process, it is imperative to understand the reaction pathway and degradation mechanisms. Kinetic studies of biomass provide information about the reaction mechanisms and pathways. Moreover, an in-depth understanding of the pyrolysis kinetics of biomass is essential for the design and optimization of thermochemical conversion reactors.<sup>[5]</sup> Furthermore, kinetic analysis is useful for mathematical modelling and the optimization of reaction conditions.<sup>[7]</sup> On the other hand, thermodynamic parameter estimation provides valuable information for energy calculations and process feasibility studies.

Although several studies have reported the pyrolysis kinetics of different agricultural residues,<sup>[8–11]</sup> to the best of the authors' knowledge, there are limited data available for the kinetics of ECR and CH. With that, the objective of this study is to investigate the thermal degradation and pyrolysis kinetics of ECR and CH by using thermogravimetric/derivative thermogravimetric analysis (TGA/DTG) analysis performed in an inert atmosphere. The iso-conversional methods of the Kissinger-Akahira-Sunose (KAS), Flynn-Wall-Ozawa (FWO), Kissinger, and Friedman method were used to estimate the kinetics parameters. The activation thermodynamic parameters, including the change in enthalpy ( $\Delta H$ ), Gibbs free energy ( $\Delta G$ ), and entropy ( $\Delta S$ ), were also evaluated. To the best

of the author's knowledge, there are minimal studies available that comprehensively evaluate the pyrolysis kinetics, thermal behaviour, and thermodynamic analysis of ECR and CH. This study provides a basis for future optimization of pyrolysis reactors and operating parameters.

## 2 | MATERIALS AND METHOD

### 2.1 | Biomass collection and preparation

ECR, together with CH, were used for TGA and evaluation of kinetic parameters. ECR was collected from a local café in Saskatoon while CH was provided by Road Coffee Inc. (SK, Canada). The collected biomass samples were air-dried in an oven for  $12 \pm 3$  hours at  $105 \pm 5^\circ\text{C}$ . To prevent the moisture adsorption of the feedstock, the dried samples were stored in an airtight container for further analysis.

### 2.2 | Proximate and ultimate analysis of biomass samples

The proximate analysis of the representative samples (ECR and CH) was carried out to determine the amount of ash content (%), moisture content (%), fixed carbon content, and volatile matter (VM%) by using the ASTM standards methods.<sup>[12–14]</sup> The ultimate analysis of ECR and CH indicates the amounts of carbon (C), hydrogen (H), sulphur (S), and nitrogen (N) in the biomass samples. The ultimate analysis was measured by using a Vario EL III CHNS elemental analyzer (Elementar Americas, Inc., Ronkonkoma, New York). The oxygen amount was evaluated as follows: ( $O\% = 100 - (C + H + N + S)$ ).

### 2.3 | Calorific value

The theoretical higher heating value (HHV) of ECR and CH were determined following Friedl's formula as shown in Equation (1)<sup>[15]</sup>:

$$\text{HHV (kJ/kg)} = (3.55 \times C^2) - (232 \times C) - (2230 \times H) + (51.2 \times C \times H) + (131 \times N) + 20\,600 \quad (1)$$

where the elemental compositions of C, H, and N are in wt%.

The experimental HHVs of ECR and CH were measured by using an oxygen bomb calorimeter (Parr 6400 Calorimeter, IL).

## 2.4 | Sample preparation for Fourier transform mid-infrared spectroscopy analysis

In order to prepare the homogenized ECR and CH samples for Fourier transform mid-infrared spectroscopy (FT-MIR) analysis, the samples were diluted with potassium bromide (KBr) to attain about 1.1%-1.3% of the overall weight of the samples. The procedure for sample preparation and FT-MIR data collection and analysis has been reported elsewhere.<sup>[16]</sup>

## 2.5 | Thermogravimetric analysis

The thermogravimetric analysis (TGA) and derivative thermogravimetric analysis (DTG) of ECR and CH were performed using a Pyris Diamond TG/DTA instrument (Perkin-Elmer, Waltham, MA). The sample weight for both precursors at each run was kept at  $12 \pm 3$  mg to mitigate the heat and mass transfer limitations. The samples were subjected to a temperature program of 25-800°C and were analyzed with a 100 mL/min flow rate N<sub>2</sub> purge gas. Different heating rates from 5-20°C/min with an interval of 5°C/min were used to elucidate the pyrolysis behaviour of ECR and CH. For each coffee residue and heating rate, three replications were performed to ensure the accuracy of the results.

## 3 | KINETIC STUDY

The obtained TGA data was used in the estimation of the kinetics parameters by using isoconversional methods

**TABLE 1** Linear equations for the isoconversional methods used to estimate the kinetics parameters

Iso-conversional model	Final equation	Notes
Kissinger-Akahira-Sunose (KAS)	$\ln\left(\frac{\beta}{T^2}\right) = \ln\left(\frac{A_0 E_A}{R g(\alpha)}\right) - \frac{E_A}{RT}$	The activation energy can be determined by the slope of $\ln(\beta/T^2)$ against $(1/T)$ for the specified value of conversion.
Flynn-Wall-Ozawa method (FWO)	$\ln(\beta) = \text{constant} - 1.052 \frac{E_A}{RT}$	A linear plot of $\ln(\beta)$ against $1/T$ would produce a slope of $-1.052 EA/R$ from which the activation energy value can be obtained.
Kissinger's Method	$\ln\left[\frac{\beta}{Tm^z}\right] = \ln\left[\frac{A_0 R}{E_A}\right] - \frac{E_A}{RTm}$	$T_m$ refers to the peak temperature obtained from the derivative thermogravimetric analysis (DTG) curve.
Friedman method	$\ln\left[\beta \frac{d\alpha}{dT}\right] = \ln[A_0 f(\alpha)] - \frac{E_A}{RT}$	Kinetic plots of $\ln\left[\beta \frac{d\alpha}{dT}\right]$ vs $1/T$ provides a slope and intercept of $-E/R$ and $\ln[A_0 f(\alpha)]$ .

such as FWO, KAS, Kissinger's method, and the Friedman method. The isoconversional methods present a reliable means of obtaining the activation energies of complex solid-state processes without any assumptions. A comparison between the model free and model fitting methods of kinetics parameter estimation is provided in section S0 of the supplementary materials (File S1). Furthermore, detail information about the derivation of each isoconversional model equations can be found in section S2 in supplementary materials (File S1). Table 1 shows the linear equations used to obtain the kinetics parameters.

## 3.1 | Evaluation of the thermodynamic parameters

The thermodynamic parameters evaluated in this study include the activation enthalpy ( $\Delta H$ ), activation entropy ( $\Delta S$ ), and Gibbs free energy ( $\Delta G$ ). Equation (S4) (File S1) refers to the Arrhenius equation that describes the relationship between rate constant of a chemical reaction and its temperature. Such relationship can also be represented by the Eyring equation:

$$k(T) = \frac{TK_B}{h} \left(\frac{1}{C^n}\right) \exp\left(\frac{-\Delta G}{RT_p}\right) \quad (2)$$

where  $C'$  represents the reference concentration of the reaction and the exponent  $n$  determines the order of reaction (0 for a first order reaction and 1 for a second order reaction).

A comparison between the Arrhenius equation (Equation (S4) in File S1) and Eyring equations (Equation (2)) provides a basis for the estimation of the thermodynamic parameters in this study, as shown in Equations (3)-(5)<sup>[17]</sup>:

$$\Delta H = E_A - RT \quad (3)$$

$$\Delta G = E_A + \ln\left(\frac{T_p K_B}{A_0 h}\right) \cdot RT \quad (4)$$

$$-\Delta S = \left(\frac{\Delta G - \Delta H}{T_p}\right) \quad (5)$$

where, from the above equations,  $K_B$  is the Boltzmann constant ( $1.381 \times 10^{-23} \text{ J} \cdot \text{K}^{-1}$ ),  $T_p$  is the peak temperature (K), and  $h$  is the Planck constant ( $6.626 \times 10^{-34} \text{ J} \cdot \text{s}$ ).

## 4 | RESULTS AND DISCUSSIONS

### 4.1 | Physicochemical properties of exhausted coffee residue and coffee husk

The proximate analysis of ECR and CH studied is presented in Table 2. It should be noted that the results of the proximate analysis were presented on an as received basis. Among the two coffee residues, ECR showed a relatively high moisture content (47.1 wt%) and volatile matter (40.4 wt%). In contrast, the ash content of CH is higher at 1.7 wt% and volatile matter (77.7 wt%). The fixed carbon contents of ECR and CH are 11.6 wt% and 17.9 wt%, respectively. The data shown in Table 2 confirm that both ECR contain very large amounts of moisture content at more than 40%. On the other hand, both samples also contain low ash content which is desirable for thermochemical conversion processes. High ash content in samples may cause fouling and disposal problems. The ultimate analysis for both ECR and CH showed a relatively high carbon content of 50 wt% and 48.5 wt%, respectively.

The amount of carbon, oxygen, and hydrogen for both feedstocks indicates their feasibility to produce green fuels and chemicals. Moreover, the low nitrogen and sulphur contents (<3%) found in both coffee residues indicates that there will be relatively low production of toxic gases such as  $\text{NO}_x$  and  $\text{SO}_x$  during pyrolysis. The experimental HHV of ECR and CH were reported as  $22.3 \text{ MJ} \cdot \text{kg}^{-1}$  and  $18.3 \text{ MJ} \cdot \text{kg}^{-1}$ , respectively. The high calorific values of both coffee residues are attributable to their lower ash and higher volatile matter content. The

**TABLE 2** Proximate, ultimate, and compositional analysis of exhausted coffee residue (ECR) and coffee husk (CH) together with their heating values

Analysis	ECR	CH
<sup>d</sup> Proximate analysis (dry basis, wt%)		
Moisture content	$47.1 \pm 0.4$	$2.7 \pm 0.05$
Volatile matter	$40.4 \pm 0.13$	$77.7 \pm 0.23$
Ash content	$0.9 \pm 0.01$	$1.7 \pm 0.01$
<sup>b</sup> Fixed carbon	$11.6 \pm 0.01$	$17.9 \pm 0.02$
Ultimate analysis (dry basis, wt%)		
C	$50.0 \pm 0.01$	$48.5 \pm 0.02$
H	$6.7 \pm 0.05$	$5.9 \pm 0.01$
N	$2.5 \pm 0.03$	$2.8 \pm 0.01$
S	$0.9 \pm 0.001$	$0.6 \pm 0.03$
<sup>a</sup> O	$39.9 \pm 0.10$	$42.2 \pm 0.01$
H/C	1.6	1.5
O/C	0.6	0.7
N/C	0.04	0.05
Empirical formula	$\text{CH}_{1.6}\text{O}_{0.6}\text{N}_{0.04}$	$\text{CH}_{1.5}\text{O}_{0.7}\text{N}_{0.05}$
Compositional analysis (wt %)		
Structural sugars	$43.3 \pm 0.4$	$39.2 \pm 0.1$
Total lignin	$32.6 \pm 0.3$	$19.6 \pm 0.1$
Higher heating value (HHV) ( $\text{MJ} \cdot \text{kg}^{-1}$ )		
Experimental HHV	22.3	18.3
<sup>c</sup> Theoretical HHV	20.4	19.6

<sup>a</sup>Oxygen (wt%) is calculated from the following equation: Oxygen (O %) =  $100 - (\text{C} + \text{H} + \text{N} + \text{S})$ .

<sup>b</sup>Fixed carbon (%) is calculated from the following equation: Fixed carbon (FC %) =  $100 - (\text{M} + \text{VM} + \text{Ash})$ .

<sup>c</sup>The theoretical HHV value was computed by Friedl's formula.

<sup>d</sup>Proximate analysis presented in the table is for the as received samples.

calorific values of ECR and CH were estimated to be higher when compared to the calorific values of agriculture waste such as rice husk ( $12.9 \text{ MJ} \cdot \text{kg}^{-1}$ ), wheat straw ( $14.7 \text{ MJ} \cdot \text{kg}^{-1}$ ), soybean straw ( $16.4 \text{ MJ} \cdot \text{kg}^{-1}$ ), rice straw ( $14.9 \text{ MJ} \cdot \text{kg}^{-1}$ ), and corn cob ( $16 \text{ MJ} \cdot \text{kg}^{-1}$ ).<sup>[18,19]</sup> The estimated HHV of ECR and CH also illustrates their suitability as feedstocks for green fuels and chemicals production through the thermochemical conversion processes. Lignin content of ECR and CH is reported as  $32.6 \pm 0.3 \text{ wt}\%$  and  $19.6 \pm 0.1 \text{ wt}\%$ , respectively. On the other hand, the structural sugar contents of CH ( $39.2 \pm 0.1 \text{ wt}\%$ ) is lower than that of ECR ( $43.3 \pm 0.4 \text{ wt}\%$ ). Details of the FTIR analysis of both coffee residues have been included in section S3 of the supplementary materials (File S1).

## 4.2 | Thermogravimetric analysis of ECR and CH

The TGA and DTG curves at constant heating rate of 10°C/min were analyzed to elucidate the pyrolytic and thermal decomposition behaviour of ECR and CH. As shown in Figure 1A,B, ECR and CH exhibit a similar devolatilization pattern with initial thermal decomposition starting at 150°C. Additionally, three different pyrolytic stages were observed. The first stage, which occurs at a temperature up to 230°C, could be attributed to the loss of moisture, decomposition of minerals, and degradation of low molecular weight compounds due to the hygroscopic nature of ECR and CH.<sup>[20]</sup> Weight loss of 4% and 3% were observed

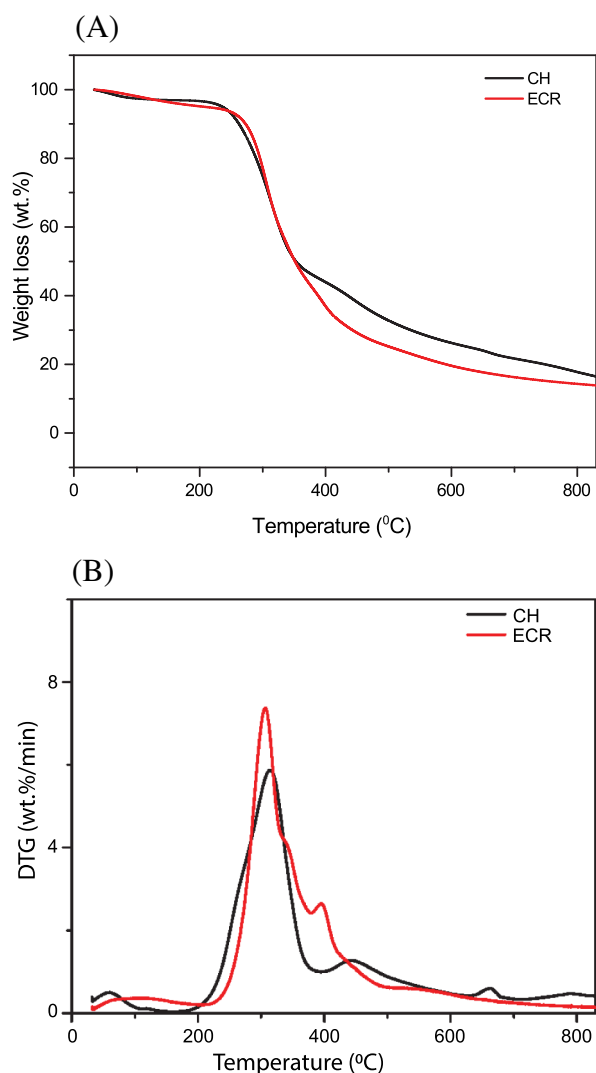


**FIGURE 1** A, thermogravimetric analysis (TGA) profiles of exhausted coffee residue (ECR) and coffee husk (CH); and B, derivative thermogravimetric analysis (DTG) profiles of ECR and CH at a constant heating rate of 10°C/min

during the first stage of the dehydration of ECR and CH, respectively.

The second stage of weight loss occurs at a higher temperature of 240–560°C for ECR and 220–550°C for CH. This stage is also known as the active pyrolytic stage. Most of the thermal decomposition occurs during the second stage with the fragmentation of higher molecular weight compounds into smaller molecular compounds. This stage is equivalent to the loss of hemicellulose, cellulose, and a small amount of lignin.

Among the two coffee residues, the highest weight loss was recorded for ECR (66%), compared to CH (59%). Owing to high volatile matter, hemicellulose, and cellulose content in ECR, the percent mass loss is higher compared to that of CH.

The last stage of thermal decomposition occurs at temperatures of 460–800°C for ECR and CH. This stage corresponds to the endothermic thermal degradation of the crystalline part of cellulose and lignin. However, the degradation rate at this stage is much slower compared to other stages and could be attributed to the recalcitrant nature of lignin, indicating that no appreciable mass conversion reactions took place in the passive pyrolytic zone. Total mass loss of 14% and 19% of the original weight was found for ECR and CH, respectively, in the passive pyrolysis zone. The percent mass loss declined for ECR compared to that of CH at the passive pyrolytic zone because of the high lignin content in it (32.6 wt%) compared to CH (19.6 wt%). Lignin is a complex polymeric substance consisting of phenylpropane molecules and highly branched C-H groups. As a result of its complex structure and recalcitrant nature, lignin is tough to degrade.

The DTG curves of ECR and CH are illustrated in Figure 1B. The DTG thermographs of the two coffee residues differ in height and peak positions. This indicates that the difference in physicochemical properties of the two coffee residues. Moreover, the distribution of the inorganic and organic components could also affect their thermal decomposition behaviour. From the DTG curves, a two-step degradation is evident for both coffee residues. The first shoulder peaks observed from the DTG curves at 220°C for ECR and 215°C for CH correspond to the decomposition of hemicellulose. It is linked with the loss of hemicellulose as it decomposes in the temperature range of 220–315°C.<sup>[19]</sup> On the other hand, the maximum peaks at around 355°C and 351°C for ECR and CH, respectively, correspond to cellulose decomposition. Cellulose undergoes thermal decomposition at temperature range of 315–450°C.<sup>[21]</sup> Finally, lignin decomposition has a broad temperature range from 200–500°C and is indicated by the peak at the flat tailing section of the DTG curves.



### 4.3 | Heating rate effect on the thermal decomposition of ECR and CH

The effect of heating rate ( $\beta$ ) on the pyrolytic behaviour of ECR and CH is shown in the TGA and DTG profiles in Figure 2. The heating rate influences the maximum peak temperature ( $T_{\text{peak}}$ ), decomposition rate, and the maximum weight loss of the samples. However, the thermal decomposition profiles of ECR and CH at all heating rates remains the same. This shows a similar degradation pattern for all heating rates. Furthermore, with elevating heating rate, the thermal decomposition is observed to approach the higher temperature zone (Figure 2B,D).

The DTG curves in Figure 2B,D indicate that the pyrolysis characteristics temperature of the active pyrolytic zone (second stage) rises with increasing heating

rate for ECR and CH. Furthermore, from Figure 3A,B, the temperature at which 5% of the sample weight is converted ( $T_{5\%}$ ) and maximum weight loss temperature ( $T_{\text{peak}}$ ) increases with elevating heating rate. Similarly, the maximum decomposition rate rose from  $3.7\text{-}15.0\% \cdot \text{min}^{-1}$  for ECR (Figure 2B) and  $3.0\text{ to }12.1\% \cdot \text{min}^{-1}$  for CH (Figure 2D). Kumar et al<sup>[22]</sup> observed similar results during the pyrolysis kinetic studies of Ru/Fe impregnated banana pseudo stem. At elevated heating rate of  $20^\circ\text{C}/\text{min}$ , the authors observed a shorter residence time for the Ru/Fe impregnated banana pseudo stem samples. Furthermore, there was an increase in the temperature required for organic matter decomposition. The authors attributed this behaviour to the low heat conductivity of biomass samples. As a result of the low heat conductivity of biomass samples, longer time is

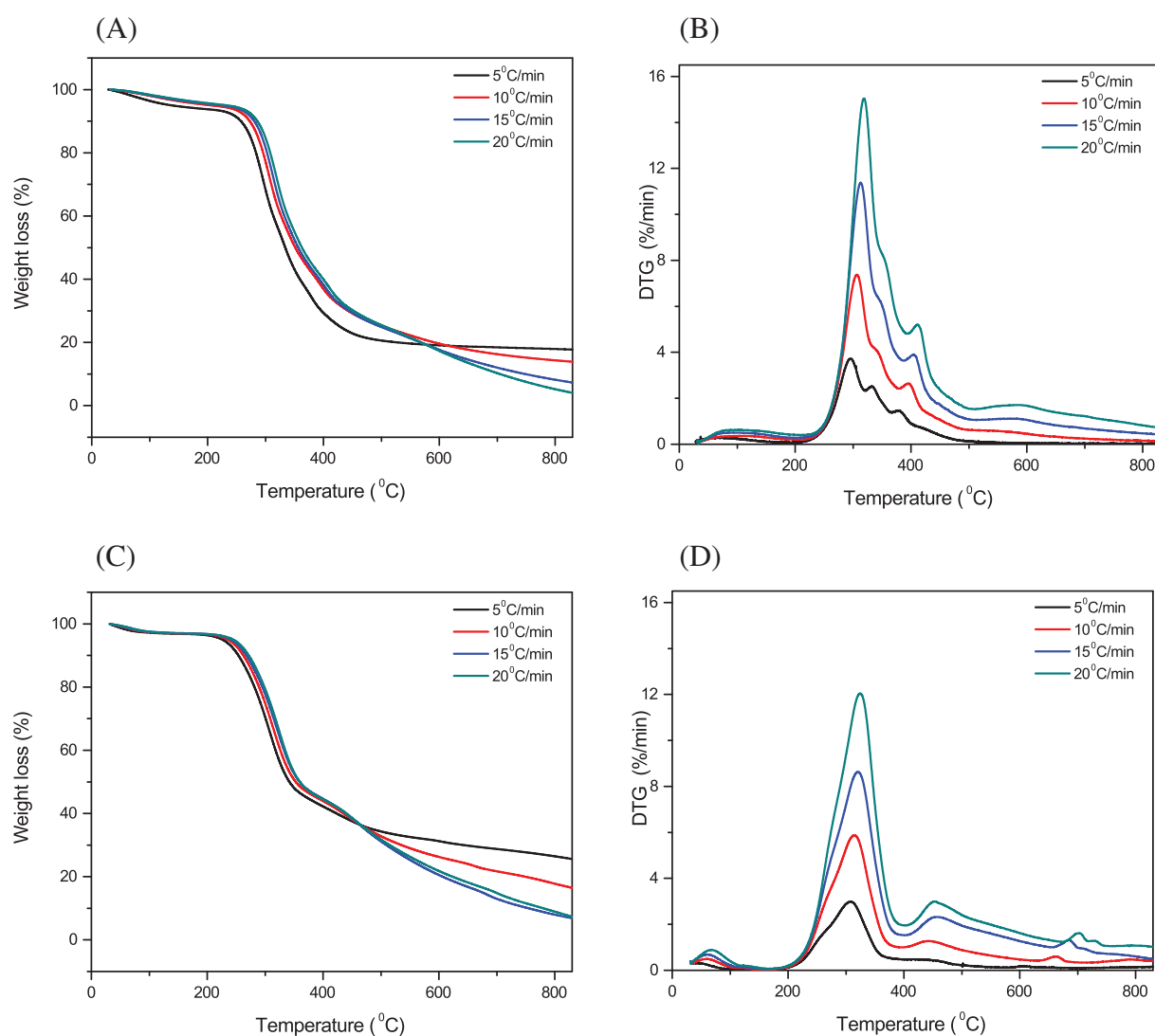


**FIGURE 2** Thermogravimetric analysis (TGA) and derivative thermogravimetric analysis (DTG) profiles of exhausted coffee residue (ECR) and coffee husk (CH) at different heating rates 5-20 °C/min: A, TGA profiles of ECR; B, DTG profiles of ECR; C, TGA profiles of CH; and D, DTG profiles of CH

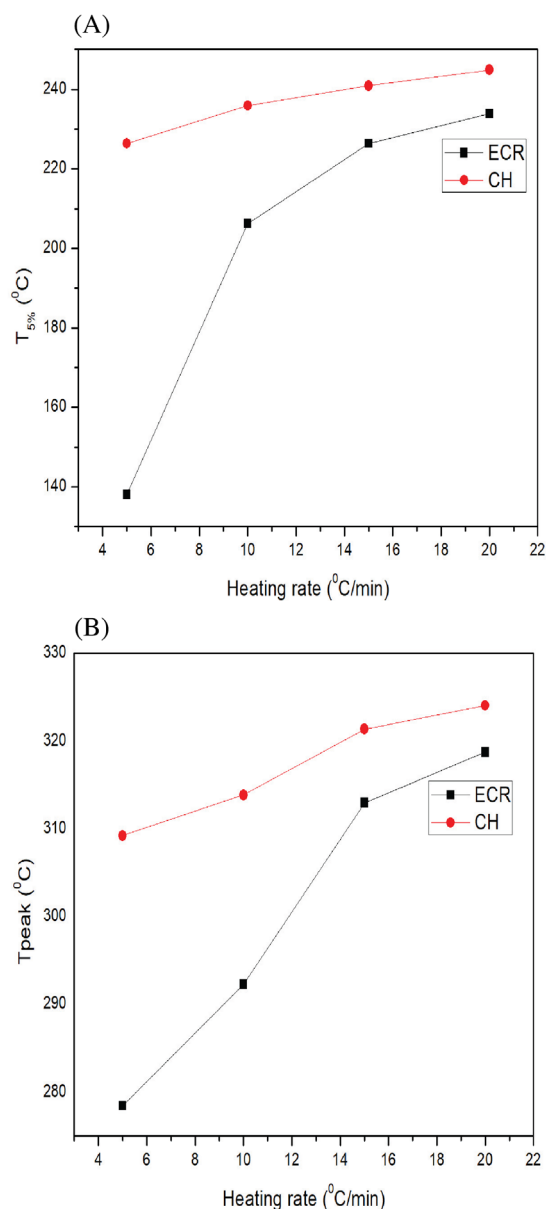


**FIGURE 3** A, effects of heating rate on the kinetics for an initial conversion of 5% for exhausted coffee residue (ECR) and coffee husk (CH); and B, effect of heating rate on the temperature at which the maximum weight loss is attained ( $T_{\text{peak}}$ ) for ECR and CH

required for heat conduction of the particle from the external surface to the interior; therefore, a temperature gradient could be formed throughout the biomass cross-section during heating.<sup>[22]</sup> However, this is not the case in our study. Pyrolysis process is controlled by kinetics together with heat and mass transfer. In the present study, we evaluated the pyrolysis kinetics using data from TGA, where a small mass (about 12 mg) of the sample were heated in a TGA analyzer.

The residual mass of the samples as well as the surrounding fluid temperature were measured over time,

with the surrounding fluid temperature assumed to be the same as the surface temperature of the sample (negligible interparticle mass transfer). However, in evaluating the pyrolysis kinetics, we assume that the mass of the sample is so small that heat transfer limitations are negligible. As a result, heat transfer limitations are not included in the model. Therefore, degradation of the biomass samples is controlled by the kinetics. Suuberg et al.<sup>[23]</sup> suggested that these heating rate effects could be as a result of the mass transport limitations. Regardless, it is important to note that in most practical applications, heat transfer limitations could still play a major role and will need to be considered.

#### 4.4 | Kinetic analysis

Figures 4 and 5 show the linear least square regression plots for FWO, KAS, and the Friedman model at progressing conversion rates. The plots of FWO and KAS models for both ECR and CH show a similar trend, while that of the Friedman model is slightly different. For both coffee residues (ECR and CH), the conversion value ranges from 0.1-0.7. It should be noted that the conversion rate lower than 0.1 and higher than 0.7 was not used in this study as a result of their non-linear characteristics and their lower correlation coefficient ( $R^2$ ) values. Moreover, all the models used in the present study showed a very good fit with the experimental data. This is verified with the value of the correlation coefficient ( $R^2$ ), which is above 0.9 at all the conversion range studied, except for the Friedman method at 0.7 conversion. The high value of the correlation coefficient also confirms the accurate prediction of the activation energy in this study.

Tables 3 and 4 depict the estimated kinetics parameters ( $E_A$  and  $A_0$ ) for ECR and CH, respectively, at different conversion (0.1-0.7). The values of activation energy are influenced by several factors such as the type of biomass, kinetics model, heating rate, and biomass particle size.<sup>[24]</sup> As shown in Tables 3 and 4, the activation energy values vary with conversion for both coffee residues. The activation energy of ECR using the FWO method was in the range of 62.3-102.4 kJ · mol<sup>-1</sup> at conversion ranges of 0.1-0.7. Likewise, the KAS and Friedman method yielded activation energy between 51.3-93.3 kJ · mol<sup>-1</sup> and 10.6-122.7 kJ · mol<sup>-1</sup>, respectively, within the same conversion range. On the other hand, CH showed higher activation values at the same conversion range (39.1-140.6 kJ · mol<sup>-1</sup> for FWO, 27.7-131.6 kJ · mol<sup>-1</sup> for KAS, and 24.9-125.9 for Friedman). The disparity in activation energies with conversion for ECR and CH could be attributed to their dissimilar pyrolysis kinetic

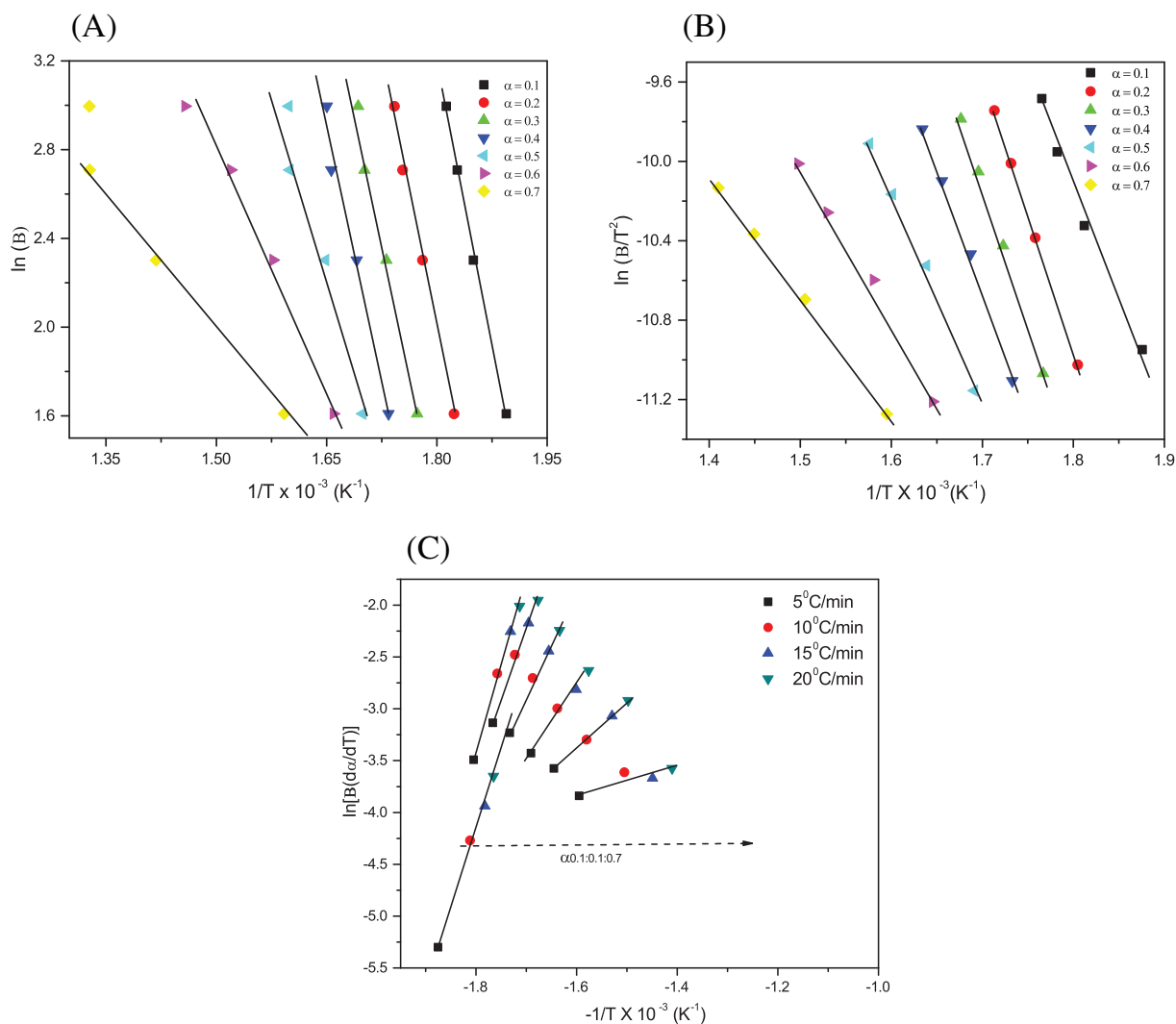


**FIGURE 4** Linear least square regression plot for exhausted coffee residue at different conversions used for the determination of activation energy by A, Flynn-Wall-Ozawa (FWO); B, Kissinger-Akahira-Sunose (KAS); and C, Friedman (the lines in C reflect the values of  $\alpha$  ranging from 0.1-0.7, starting from left to right)

behaviour and percentage of cellulose, hemicellulose, and lignin present in these materials, together with their collective interactions.<sup>[17]</sup> Fixed carbon content and volatile matter also play a major role in the variation in the activation energies for the two samples. Furthermore, since the activation energy of biomass is strongly dependent on the pyrolysis mechanism, it could be stated that both ECR and CH exhibit different reaction mechanisms during pyrolysis. Kaur et al<sup>[17]</sup> reported similar observations using castor oil as feedstock. In another study by Ashraf et al,<sup>[9]</sup> the authors reported the activation energies of two coals (Dukki coal (DC) and Chamalang coal (CC)) and four different agricultural residues (corn husk (CU), falsa stick (FS), rice husk (RH,) and sunflower disc (SD)). The activation energies were in the order of  $CC < DC < SD < RH < FS < CU$ .<sup>[25]</sup> The authors attributed the high activation energy of corn husk to its low

volatile matter and high fixed carbon contents compared to coal and other agricultural residues.

The variation of activation energy with conversion estimated from the Friedman, KAS, and FWO methods is further illustrated in Figure S1 (File S1). The dependency of activation energy with conversion for both ECR and CH indicates that the reaction mechanism is not the same in the whole decomposition process.<sup>[26-28]</sup> As proposed by Vyazovkin et al,<sup>[28]</sup> most of the thermally initiated processes exhibit a characteristic activation energy vs conversion dependencies. These variations can be used for predicting kinetics and exploring the process mechanism. If the activation energy is constant over the entire conversion range, then it is likely that the process is a single reaction step dominated process. However, in most processes, the activation energy varies largely with conversion, which is the same with the present study, where



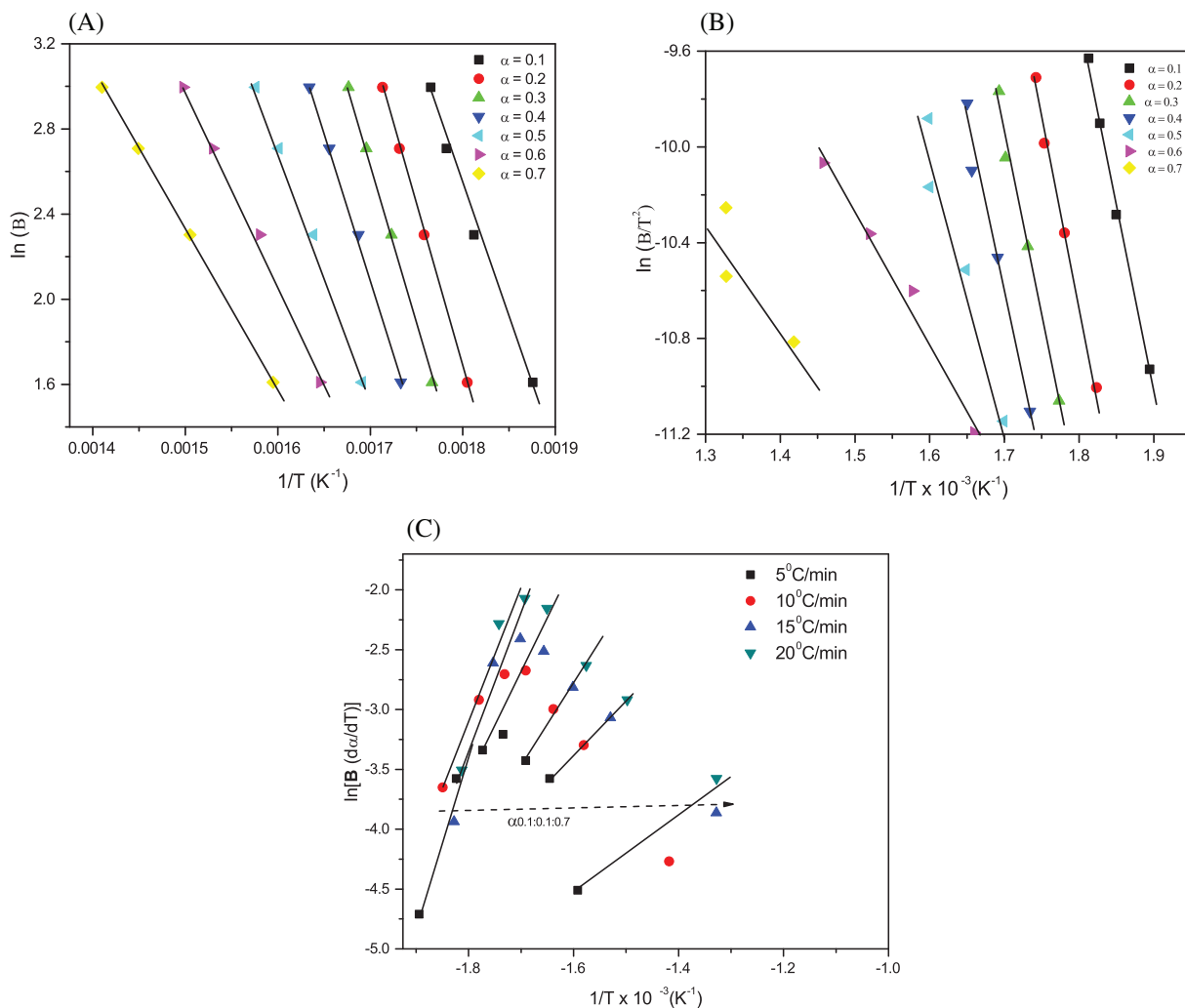


**FIGURE 5** Linear least square regression plot for coffee husk (CH) at different conversions used for the determination of activation energy by A, Flynn-Wall-Ozawa (FWO); B, Kissinger-Akahira-Sunose (KAS); and C, Friedman (the lines in C reflect the values of  $\alpha$  ranging from 0.1-0.7, starting from left to right)

**TABLE 3** The kinetic parameters obtained from iso-conversional method using the fitted equation for exhausted coffee residue (ECR)

Feedstock: ECR									
$\alpha$	FWO method			KAS method			Friedman method		
	$E_A$ ( $\text{kJ} \cdot \text{mol}^{-1}$ )	$A$ ( $\text{s}^{-1}$ )	$R^2$	$E_A$ ( $\text{kJ} \cdot \text{mol}^{-1}$ )	$A$ ( $\text{s}^{-1}$ )	$R^2$	$E_A$ ( $\text{kJ} \cdot \text{mol}^{-1}$ )	$A$ ( $\text{s}^{-1}$ )	$R^2$
0.1	102.4	$1.1 \times 10^9$	0.9924	93.3	$1.5 \times 10^8$	0.9911	122.7	$1.1 \times 10^{11}$	0.9957
0.2	125.2	$1.8 \times 10^{11}$	0.9998	115.8	$2.2 \times 10^{10}$	0.9998	134.9	$1.5 \times 10^{12}$	0.9967
0.3	127.7	$3.1 \times 10^{11}$	0.9998	118.1	$3.6 \times 10^{10}$	0.9997	109.1	$4.9 \times 10^9$	0.9942
0.4	116.1	$2.3 \times 10^{10}$	0.9983	106.1	$2.6 \times 10^9$	0.9979	82.4	$1.3 \times 10^7$	0.9937
0.5	99.7	$6.1 \times 10^8$	0.9976	89.5	$6.3 \times 10^7$	0.9969	56.3	$3.4 \times 10^4$	0.9893
0.6	77.4	$4.1 \times 10^6$	0.9956	66.8	$3.7 \times 10^5$	0.9938	36.9	$3.6 \times 10^2$	0.9997
0.7	62.3	$1.3 \times 10^5$	0.9998	51.3	$1.1 \times 10^4$	0.9995	10.6	$3.8 \times 10^1$	0.7596
<b>Average</b>	<b>101.6</b>	<b><math>7.2 \times 10^{10}</math></b>	-	<b>91.6</b>	<b><math>8.7 \times 10^9</math></b>	-	<b>90.4</b>	<b><math>2.3 \times 10^{11}</math></b>	-

Abbreviations: FWO, Flynn-Wall-Ozawa method; KAS, Kissinger-Akahira-Sunose.

for both ECR and CH the activation energy values ranges from 10-140 kJ/mol.

The iso-conversional method describes the kinetics of a process with the aid of a multiple single-step kinetics equation with each one of them related to a certain extent of conversion. Therefore, a reaction with activation energy against conversion dependence indicates the

presence of a complex multistep mechanism. The nature of such a reaction can be determined by the shape of the activation energy vs conversion curves. In the present study, the curve is complex and convoluted with multiple peaks. As noted by several authors,<sup>[10,23,27-29]</sup> the presence of several peaks and convolutions in the curve could be attributed to the difference in the thermal

**TABLE 4** The kinetic parameters obtained from iso-conversional method using the fitted equation for coffee husk (CH)

CH									
$\alpha$	FWO method			KAS method			Friedman method		
	$E_A$ (kJ · mol <sup>-1</sup> )	A (s <sup>-1</sup> )	R <sup>2</sup>	$E_A$ (kJ · mol <sup>-1</sup> )	A (s <sup>-1</sup> )	R <sup>2</sup>	$E_A$ (kJ · mol <sup>-1</sup> )	A (s <sup>-1</sup> )	R <sup>2</sup>
0.1	140.6	$1.6 \times 10^{12}$	0.997	131.6	$2.4 \times 10^{11}$	0.9966	111.2	$3.1 \times 10^9$	0.7814
0.2	138.0	$9.3 \times 10^{11}$	0.995	128.7	$1.3 \times 10^{11}$	0.9943	125.9	$7.0 \times 10^{10}$	0.9858
0.3	136.7	$6.9 \times 10^{11}$	0.9899	127.1	$9.1 \times 10^{10}$	0.9884	121.3	$2.6 \times 10^{10}$	0.9713
0.4	128.4	$1.2 \times 10^{11}$	0.9826	118.6	$1.5 \times 10^{10}$	0.9797	90.4	$3.1 \times 10^7$	0.9205
0.5	102.7	$4.9 \times 10^8$	0.9626	92.6	$5.7 \times 10^7$	0.9543	80.0	$3.7 \times 10^6$	0.9124
0.6	57.7	$2.8 \times 10^4$	0.9829	45.9	$1.9 \times 10^3$	0.9823	77.0	$1.9 \times 10^6$	0.971 54
0.7	39.1	$4.1 \times 10^2$	0.9517	27.7	$2.8 \times 10^1$	0.9102	24.9	$1.4 \times 10^1$	0.8087
<b>Average</b>	<b>106.2</b>	<b><math>4.8 \times 10^{11}</math></b>		<b>96.0</b>	<b><math>6.7 \times 10^{10}</math></b>		<b>100.9</b>	<b><math>1.4 \times 10^{10}</math></b>	

Abbreviations: FWO, Flynn-Wall-Ozawa method; KAS, Kissinger-Akahira-Sunose.

**TABLE 5** Comparison of coffee residues activation energies ( $E_A$ ) calculated with FWO method (present work) with  $E_A$  of various biomass resources reported in the literature

Biomass	Proximate analysis (wt%) (dry basis)		Ultimate analysis (wt%) (dry basis)					$E_A$ (kJ · mol <sup>-1</sup> )			Reference
	Ash (wt%)	Moisture (wt%)	C	H	N	S	O	FWO method	KAS method	Friedman	
Exhausted coffee residue (ECR)	0.9	3.3	50	6.7	2.5	0.9	39.9	102.4	91.6	90.4	Present Work
Coffee husk (CH)	1.7	2.7	48.5	5.9	2.8	0.6	40.6	140.6	96.0	100.9	Present work
Corn stalk	15.9	-	48.8	6.6	3.7	-	40.9	-	-	473	Cai et al <sup>[30]</sup>
Hazelnut husk	5.3	7.2	42.6	5.5	1.1	0.13	50.6	162.1	162.6	-	Ceylan and Topçu <sup>[31]</sup>
Raw rice straw (RRS)	-	-	-	-	-	-	-	200.8	-	-	Sheng et al <sup>[32]</sup>
Palm kernel shell	2.8	12.7	51.6	6.3	0.7	0.1	41.3	262	-	-	Ma et al. <sup>[24]</sup>
Pine sawdust	2.07	6.1	50.3	6	0.7	-	43	191	-	-	Cruz and Crnkovic <sup>[33]</sup>
Sal sawdust	1.1	8.9	49.8	6	0.6	-	43.6	175	-	-	Mishra and Mohanty <sup>[5]</sup>
Areca nut husk	2.5	7.4	48.8	5.8	2	0.1	43.5	196	-	-	Mishra Mohanty <sup>[5]</sup>
Castor residue	5.4	11.1	43.6	5.6	4.7	-	46.2	215.6	-	-	Kaur et al <sup>[17]</sup>

Abbreviations: FWO, Flynn-Wall-Ozawa method; KAS, Kissinger-Akahira-Sunose.

decomposition behaviour of several components of biomass (cellulose, hemicellulose, and lignin). Each component exhibits different decomposition temperature and at varying stages of conversion. As confirmed by the FTIR analysis, ECR and CH contain several components with different functional groups and show different thermal decomposition behaviour.

The average value of activation energy reported in this study has a meaning of a single parameter that is linked to the activation energies of individual decomposition process of several biopolymers present in the lignocellulosic biomass sample. The average activation energies for both feedstocks were found to be lower compared to the activation energies of several feedstocks reported in Table 5 (eg, palm kernel shell,  $262 \text{ kJ} \cdot \text{mol}^{-1}$ <sup>[24]</sup>; hazelnut husk,  $162.1 \text{ kJ} \cdot \text{mol}^{-1}$ <sup>[31]</sup>; castor,  $215.6 \text{ kJ} \cdot \text{mol}^{-1}$ <sup>[17]</sup>; and raw rice straw,  $200.8 \text{ kJ} \cdot \text{mol}^{-1}$ <sup>[32]</sup>). Activation energy is an essential criterion for the determination of fuel reactivity.<sup>[34]</sup> Since fuel reactivity plays a significant role in gasification and pyrolysis, it is crucial to understand the extent and relationship between activation energy and conversion during pyrolysis. It is almost impossible to start reactions with high activation energy, as increased value demonstrates that the rate of reaction is slow. Low activation energy is desirable, therefore ECR is seen as a superior fuel when compared with CH and other biomass samples listed in Table 5.

#### 4.5 | Thermodynamic parameters estimation

Thermodynamic estimation provides information on the variation of enthalpy ( $\Delta H$ ,  $\text{kJ/mol}$ ), entropy ( $\Delta S$ ,  $\text{J} \cdot \text{mol}^{-1}$ ), and Gibbs energy ( $\Delta G$ ,  $\text{kJ/mol}$ ) with conversion. It is important to note that the thermodynamic parameters evaluated in this study are the activation thermodynamic parameters; therefore, they are only associated with the activation process and not the entire process.

Enthalpy is a chemical reaction state function that helps to identify whether heat is absorbed or released in a reaction.<sup>[10]</sup> Enthalpy also represents the total heat content of a system. The changes in enthalpy ( $\Delta H$ ) with conversion for ECR and CH are presented in Tables S1 and S2 (File S1). For all three iso-conversional methods, a slight deviation in enthalpy values with increasing conversion could be attributed to the difference in energy between the reactants and the activated complex. The lower the energy difference, the higher the tendency to form the activated complex.<sup>[25]</sup> The average enthalpy obtained using the KAS, FWO, and Friedman methods

was reported as  $91.1 \text{ kJ} \cdot \text{mol}^{-1}$ ,  $101.3 \text{ kJ} \cdot \text{mol}^{-1}$ , and  $85.2 \text{ kJ} \cdot \text{mol}^{-1}$ , respectively, for CH. On the contrary, ECR has a lower average enthalpy value of  $86.9 \text{ kJ} \cdot \text{mol}^{-1}$  (KAS),  $99.1 \text{ kJ} \cdot \text{mol}^{-1}$  (FWO), and  $76.6 \text{ kJ} \cdot \text{mol}^{-1}$  (Friedman). The highest  $\Delta H$  value was obtained at conversion ranges of 0.1-0.3 for both feedstocks (Figure 6A,B). The superior value of  $\Delta H$  at low conversion ranges (0.1-0.3) could be attributed to the fact that lower conversions are attained at lower temperature. However, it is important to note that the ability of a pyrolysis reaction to occur at lower or higher temperatures is determined by both the frequency factor and activation energy.

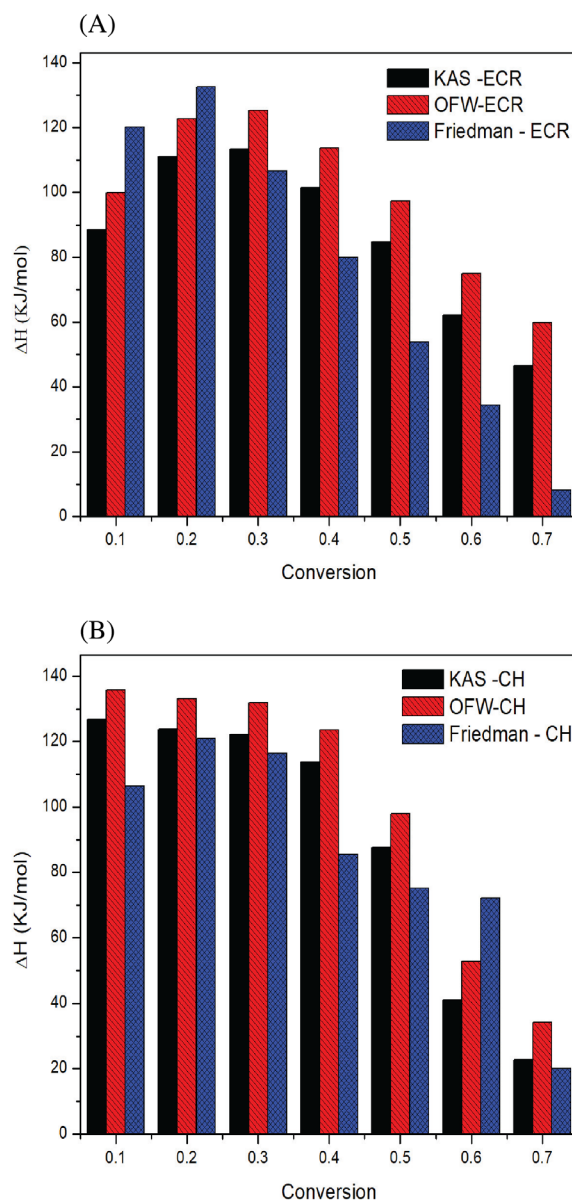


**FIGURE 6** Change in activation enthalpy with conversion for different iso-conversional methods for A, exhausted coffee residue (ECR); and B, coffee husk (CH)

The entropy of a system measures the degree of randomness or disorderliness of the reacting system. It was observed from Table S1 (File S1) that the entropy values for both ECR and CH are negative for all the fractional conversions from 0.1-0.7. Although negative value of entropy implies that the degree of randomness of the products from bond dissociation is less than that of the starting reactants (ie, a decrease in the degree of randomness or disorderliness of the system), that is usually not the case in decomposition reactions such as pyrolysis. During pyrolysis, organic components undergo thermal decomposition in the absence of oxygen to produce gases, chars, and bio-oils depending on the reaction conditions. Therefore, the negative value of entropy in this study could be a result of its association with the formation of the activated complex.

## 5 | CONCLUSIONS

The pyrolysis kinetics of ECR and CH were comprehensively studied using TGA data. Iso-conversional approaches such as the Kissinger, KAS, FWO, and Friedman method were used to calculate the kinetic parameters. Activation thermodynamic variables such as enthalpy, entropy, and Gibbs free energy, were also evaluated. TGA analysis of the two samples shows that the degradation pattern of ECR and CH exists in three different stages of weight loss. The first stage is attributed to the loss of moisture and volatile components. The second stage of weight loss stage corresponds to the loss of holocelluloses (cellulose and hemicellulose). The last stage at higher temperatures is attributed to the lignin decomposition and char formation. The average activation energies calculated for ECR were  $101.6 \text{ kJ} \cdot \text{mol}^{-1}$  (FWO method),  $91.56 \text{ kJ} \cdot \text{mol}^{-1}$  (KAS method), and  $90.4 \text{ kJ} \cdot \text{mol}^{-1}$  (Friedman method). For CH, the average activation energies were  $106.2 \text{ kJ} \cdot \text{mol}^{-1}$  (FWO method),  $96.0 \text{ kJ} \cdot \text{mol}^{-1}$  (KAS method), and  $101 \text{ kJ} \cdot \text{mol}^{-1}$  (Friedman method). Higher volatile content (81.2 wt%), high heating value (22.3 MJ/mol), lower activation energy ( $90.4\text{-}101.6 \text{ kJmol}^{-1}$ ), Gibbs free energy ( $146.11\text{-}148.35 \text{ kJ} \cdot \text{mol}^{-1}$ ), entropy ( $-127 \text{ J} \cdot \text{mol}^{-1}$ ), and lower content of N (2.3 wt%) and S (0.9 wt%) of ECR compared to CH have shown that it has higher potential for bioenergy production.

## ACKNOWLEDGEMENTS

The authors would like to gratefully acknowledge the financial support received from the Natural Sciences and Engineering Research Council of Canada (NSERC) and Canada Research Chair (CRC) program towards completion of the current research work. Part of the research described here

was performed at the Canadian Light Source (CLS, SK). The authors also express their sincere gratitude to Dr. Sonil Nanda for sharing technical knowledge and time for discussion during the drafting of the manuscript.

## NOMENCLATURE

F( $\alpha$ )	reaction model
AC	ash content
CH	coffee husk
DTA	differential thermogravimetry analysis
DTG	derivative thermogravimetric analysis
E <sub>A</sub> ,	activation energy
ECR	exhausted coffee residue
FC	fixed carbon
HHV	higher heating value
k(T)	temperature dependent rate constant
KAS	Kissinger-Akahira-Sunose method
MC	moisture content
FWO	Flynn-Wall-Ozawa method
R	universal gas constant
T	temperature dependent rate constant
T <sub>5%</sub>	initial decomposition temperature
TGA	thermogravimetric analysis
T <sub>mp</sub>	peak temperature obtained from the DTG
T <sub>peak</sub>	temperature at which maximum weight loss occurs from DTG curve
VM	volatile matter
$\alpha$	conversion
$\beta$	heating rate
A	frequency factors

## PEER REVIEW

The peer review history for this article is available at <https://publons.com/publon/10.1002/cjce.24037>.

## REFERENCES

- [1] V. Aristizábal-Marulanda, Y. Chacón-Perez, C. A. Cardona Alzate, in *Handbook of Coffee Processing by-Products: Sustainable Applications* (Ed: C. Galanakis), Elsevier Inc., San Diego, CA **2017**, p. 63.
- [2] S. I. Mussatto, E. M. S. Machado, S. Martins, J. A. Teixeira, *Food Bioprocess Tech.* **2011**, *4*, 661.
- [3] B. Janissen, T. Huynh, *Resour. Conserv. Recycl.* **2018**, *128*, 110.
- [4] J. A. Okolie, R. Rana, S. Nanda, A. K. Dalai, J. A. Kozinski, *Sustainable Energy Fuels.* **2019**, *3*, 578.
- [5] R. K. Mishra, K. Mohanty, *Bioresour. Technol.* **2018**, *251*, 63.
- [6] M. Hu, Z. Chen, S. Wang, D. Guo, C. Ma, Y. Zhou, J. Chen, M. Laghari, S. Fazal, B. Xiao, B. Zhang, S. Ma, *Energ. Convers. Manage.* **2016**, *118*, 1.
- [7] S. A. El-Sayed, M. E. Mostafa, *Energ. Convers. Manage.* **2014**, *85*, 165.
- [8] M. S. Ahmad, M. A. Mehmood, O. S. Al Ayed, G. Ye, H. Luo, M. Ibrahim, U. Rashid, I. Arbi Nehdi, G. Qadir, *Bioresour. Technol.* **2017**, *224*, 708.
- [9] A. Ashraf, H. Sattar, S. Munir, *Fuel* **2019**, *235*, 504.

- [10] V. Dhyani, T. Bhaskar, in *Waste Biorefinery* (Eds: T. Bhaskar, A. Pandey, S. V. Mohan, D.-J. Lee, S. K. Khanal), Elsevier, San Diego, CA **2018**, p. 39.
- [11] E. Biagini, F. Barontini, L. Tognotti, *Can. J. Chem. Eng.* **2017**, 95, 913.
- [12] *Standard Method for Volatile Matter in the Analysis Sample of Coal and Coke*, ASTM D3175-11, ASTM International, West Conshohocken, PA **2011**. <https://doi.org/10.1520/D3175-11>.
- [13] ASTM, *Annual Book of ASTM Standards*, ASTM International, West Conshohocken, PA **2004**, p. 3.
- [14] *Standard Test Method for Moisture Analysis of Particulate Wood Fuels*, ASTM E871-82, ASTM International, West Conshohocken, PA **2006**. <https://doi.org/10.1520/E0871-82R06>.
- [15] A. Friedl, E. Padouvas, H. Rotter, K. Varmuza, *Anal. Chim. Acta* **2005**, 544, 191.
- [16] C. Karunakaran, P. Vijayan, J. Stobbs, R. K. Bamrah, G. Arganosa, T. D. Warkentin, *Food Chem.* **2020**, 309, 125585.
- [17] R. Kaur, P. Gera, M. K. Jha, T. Bhaskar, *Bioresource Technol.* **2018**, 250, 422.
- [18] J. A. Okolie, S. Nanda, A. K. Dalai, J. A. Kozinski, *Energ. Convers. Manage.* **2020**, 208, 112545.
- [19] B. Biswas, N. Pandey, Y. Bisht, R. Singh, J. Kumar, T. Bhaskar, *Bioresource Technol.* **2017**, 237, 57.
- [20] D. Mallick, M. K. Poddar, P. Mahanta, V. S. Moholkar, *Bioresource Technol.* **2018**, 261, 294.
- [21] R. Soysa, Y. S. Choi, S. J. Kim, S. K. Choi, *Int. J. Hydrogen Energ.* **2016**, 41, 16436.
- [22] A. Kumar, S. V. P. Mylapilli, S. N. Reddy, *Bioresource Technol.* **2019**, 285, 121318.
- [23] E. M. Suuberg, I. Milosavljevic, V. Oja, *Symp. (Int.) Combust.* **1996**, 26, 1515.
- [24] Z. Ma, D. Chen, J. Gu, B. Bao, Q. Zhang, *Energ. Convers. Manage.* **2015**, 89, 251.
- [25] L. T. Vlaev, V. G. Georgieva, S. D. Genieva, *J. Therm. Anal. Calorim.* **2007**, 88, 805.
- [26] S. Vyazovkin, N. Sbirrazzuoli, *Macromol. Rapid Commun.* **2006**, 27, 1515.
- [27] S. Vyazovkin, C. A. Wight, *Thermochim. Acta* **1999**, 340–341, 53.
- [28] S. Vyazovkin, A. K. Burnham, J. M. Criado, L. A. Pérez-Maqueda, C. Popescu, N. Sbirrazzuoli, *Thermochim. Acta* **2011**, 520, 1.
- [29] A. Aboulkas, K. El harfi, A. El Bouadili, *Energ. Convers. Manage.* **2010**, 51, 1363.
- [30] J. Cai, D. Xu, Z. Dong, X. Yu, Y. Yang, S. W. Banks, A. V. Bridgwater, *Renew. Sust. Energ. Rev.* **2018**, 82, 2705.
- [31] S. Ceylan, Y. Topçu, *Bioresource Technol.* **2014**, 156, 182.
- [32] J. Sheng, D. Ji, F. Yu, L. Cui, Q. Zeng, N. Ai, J. Ji, *IERI Procedia* **2014**, 8, 30.
- [33] G. Cruz, P. M. Crnkovic, *J. Therm. Anal. Calorim.* **2016**, 123, 1003.
- [34] C. Gai, Y. Dong, T. Zhang, *Bioresource Technol.* **2013**, 127, 298.

### SUPPORTING INFORMATION

Additional supporting information may be found online in the Supporting Information section at the end of this article.

**How to cite this article:** Mukherjee A, Okolie JA, Tyagi R, Dalai AK, Niu C. Pyrolysis kinetics and activation thermodynamic parameters of exhausted coffee residue and coffee husk using thermogravimetric analysis. *Can J Chem Eng.* 2021; 99:1683–1695. <https://doi.org/10.1002/cjce.24037>